

## Force between static quarks

D. Barkai

*Control Data Corporation at the Institute for Computational Studies at Colorado State University,  
P.O. Box 1852 Fort Collins, Colorado 80522*

K. J. M. Moriarty\*

*Idaho National Engineering Laboratory, Idaho Falls, Idaho 83415*

C. Rebbi

*Department of Physics, Brookhaven National Laboratory, Upton, New York 11973*

(Received 2 March 1984)

We present Monte Carlo results for the force between static quarks, calculated on a large ( $16^3 \times 32$ ) lattice. A simulation with high statistics allows us to compute expectation values for loop factors of size up to  $8 \times 8$  at several values of  $\beta$  in the transition region. Values and errors are tabulated; a fitting procedure is then used to evaluate the force between static quarks and, in particular, its asymptotic limit, i.e., the string tension  $\sigma$ . We find good agreement with scaling for  $\beta \geq 6$ , with a ratio between scale parameter  $\Lambda$  and  $\sqrt{\sigma}$  approximately equal to  $9.6 \times 10^{-3}$ .

### I. INTRODUCTION

One of the most important goals of quantum chromodynamics, the gauge theory of strong interactions, is to establish that quarks are permanently bound within hadrons. In particular, one wants to determine the value of the string tension, i.e., the asymptotic value taken by the attractive force between static quarks at very large separation, relating it to whatever scale parameter one uses in the renormalization procedure. Once this is achieved, any other calculable dimensional quantity can be expressed in terms of the string tension, whose phenomenological value is approximately  $(420 \text{ MeV})^2$ . A determination of the force between static quarks at nonasymptotic separations is also of great theoretical and phenomenological interest.

Monte Carlo simulations of lattice gauge systems<sup>1</sup> constitute a very powerful tool for computing the quantities mentioned above and several other observables of the theory of strong interactions. In particular, Monte Carlo simulations gave the first compelling, albeit numerical, evidence that non-Abelian gauge theories confine<sup>2</sup> and are, up to date, the only method to evaluate QCD observables of nonperturbative nature directly from first principles, with no intervening phenomenological assumption. Many Monte Carlo calculations of the string tension  $\sigma$ , in units of the lattice spacing  $a$ , and of the ratio  $\Lambda/\sqrt{\sigma}$  ( $\Lambda$  being the lattice scale parameter) have already been published.<sup>3</sup> However, inconsistencies between various Monte Carlo (MC) results indicate that the small overall volume of the lattice and insufficient statistics may induce substantial errors in the determination of the observables. This is put in particular evidence by the fact that whereas the early MC calculations of  $\Lambda/\sqrt{\sigma}$  produced numbers of the order of  $6 \times 10^{-3}$  for this ratio, values as high as  $12 \times 10^{-3}$  were found necessary to obtain agreement with results for the lowest masses in the hadronic spectrum, when the latter calculation was performed on a reasonably large lattice.<sup>4</sup>

Notice that an increase of  $\Lambda$  by a definite factor implies a corresponding reduction of the value of the lattice spacing  $a$  at a given value of the coupling parameter  $\beta$ .  $a$ ,  $\beta$ , and  $\Lambda$  are related by

$$a = \frac{1}{\Lambda} \left[ \frac{8\pi^2\beta}{33} \right]^{51/121} \exp \left[ -\frac{4\pi^2\beta}{33} \right] [1 + O(1/\beta)], \quad (1.1)$$

in the SU(3) lattice gauge theory,  $\beta$  being in turn related to the bare coupling constant  $g$  by

$$\beta = \frac{6}{g^2}. \quad (1.2)$$

Insofar as the string tension can be considered a rather well-established phenomenological parameter from hadronic spectroscopy, an accurate determination of  $\Lambda/\sqrt{\sigma}$  becomes extremely important, because it provides an absolute scale against which to compare whatever other dimensional observable one may be able to calculate. In this paper we report the results of a calculation of the string tension and, more generally, of the force between static quarks on a large lattice ( $16^3 \times 32$ ) and with high statistics.

Within the scope of a general program to utilize the computational capabilities of the most powerful modern vector processors for a variety of Monte Carlo simulations, we have developed a code<sup>5</sup> that can upgrade an SU(3) link variable in 41  $\mu\text{sec}$  (on a CDC CYBER 205, for technical details see Ref. 5). The upgrade of the 524 288 dynamical variables [i.e., SU(3) matrices] on a  $16^3 \times 32$  lattice then requires only 21.5 sec and Monte Carlo simulations involving hundreds or thousands of iterations through that size lattice become feasible. Thus, after an equilibration procedure which we describe in the next section, we have measured expectation values of loop factors over runs of 1000 iterations at each of 6 values of

$\beta$ , equally spaced from 5.6 to 6.6. The results, as well as our inferences for the force between static quarks and the string tension, are reported here. The final configurations of the runs, which are presumed to be well thermalized, are preserved for further analyses, about which we hope to report in future publications.

In Sec. II we present our results. These ought to be divided into two categories. Six tables list the values found for the expectation values of the loop factors for loops up to  $8 \times 8$  and the corresponding statistical errors, as well as some suitable combinations of logarithms of the above, which are useful to determine the force, and corresponding errors. That much of our results is of rather objective nature. We would be surprised if any correct Monte Carlo simulation on a lattice of size equal to or larger than the one we have been considering produced results inconsistent with those we quote in the tables. The estimate of the force and of the string tension from the expectation values of loop factors is instead more subjective, because in either case one must extrapolate to infinite-size quantities, which the Monte Carlo simulation can give only for finite size. We apply an extrapolation procedure which appears to give sensible results, but we acknowledge that numbers differing by more than statistical fluctuations could be obtained by researchers using a different method of extrapolation. Section III is devoted to a discussion of programming details and of the error analysis. A few concluding remarks are presented in Sec. IV.

## II. RESULTS

It is useful to establish our notation. We denote lattice sites by vectors  $x$  with integer-valued components, directions by superscripts  $\mu, \nu, \dots$ , and displacements of one lattice spacing in the  $\mu$  direction by  $\hat{\mu}$ . The dynamical variables are SU(3) matrices  $U_x^\mu$  assigned to the oriented links,  $x$  to  $x + \hat{\mu}$ , of the lattice. We define transport operators for rectangular loops of size  $i, j$  in the  $\mu, \nu$  plane:

$$U_{x,ij}^{\mu\nu} = U_x^{\nu\dagger} \cdots U_{x+(j-1)\hat{\nu}}^{\nu\dagger} U_{x+j\hat{\nu}}^{\mu\dagger} \cdots U_{x+(i-1)\hat{\mu}+j\hat{\nu}}^{\mu\dagger} \\ \times U_{x+i\hat{\mu}+(j-1)\hat{\nu}}^{\nu} \cdots U_{x+i\hat{\mu}}^{\nu} U_{x+(i-1)\hat{\mu}}^{\mu} \cdots U_x^{\mu} \quad (2.1)$$

and Wilson loop factors

$$w_{x,ik}^{\mu\nu} = \frac{1}{3} \text{Re Tr } U_{x,ij}^{\mu\nu}. \quad (2.2)$$

The action is given by

$$S = \beta \sum_{x,\mu < \nu} (1 - w_{x,11}^{\mu\nu}). \quad (2.3)$$

We further represent by  $w_{ij}^{\mu\nu}$  the average value of  $w_{x,ij}^{\mu\nu}$  over a definite gauge field configuration and by  $W_{ij}$  the average value over spatial directions of  $w_{ij}^{\mu\nu}$ :

$$w_{ij}^{\mu\nu} = \frac{1}{N} \sum_x w_{x,ij}^{\mu\nu}, \quad (2.4)$$

$$w_{ij} = \frac{1}{6} \sum_{\substack{\mu \neq \nu \\ \mu, \nu \leq 3}} w_{ij}^{\mu\nu}, \quad (2.5)$$

$N$  being the number of points in the lattice. (For technical reasons, which will be explained in Sec. III, we limit our averages to loops having both sides in spatial direc-

tions.) Finally, angular brackets will represent averages taken over the many configurations generated during a Monte Carlo simulation at a definite value of  $\beta$ . Thus,  $\langle W_{ij} \rangle$  will denote the numerical result obtained in our calculation, which, of course, is the best approximation we can achieve to the correct quantum-mechanical expectation value of the Wilson loop factor itself.

The Monte Carlo simulation has been done as follows. 1000 iterations were performed on a lattice of  $16^4$  points at  $\beta=5.6$  working from a cold start with all  $U_x^\mu = I$ , obtaining a final configuration  $C_1$ .  $C_1$  was used as the initial configuration for a run of 500 iterations at  $\beta=5.8$ , obtaining a final configuration  $C_2$ , which was then used as the initial configuration for the simulation at  $\beta=6.0$ , etc. In this way, 6 configurations,  $C_1, \dots, C_6$ , corresponding to  $\beta=5.6, 5.8, 6.0, 6.2, 6.4, 6.6$ , thermalized by at least 500 MC iterations plus those performed at the lower  $\beta$  values, were generated for a  $16^4$  lattice. At this point configurations  $C'_1, \dots, C'_6$  on a  $16^3 \times 32$  lattice were obtained by duplicating the configurations  $C_1, \dots, C_6$  in the time directions. 100 further thermalizing iterations were made at each value of  $\beta$ , followed by 1000 iterations in the course of which all Wilson loop factors corresponding to rectangles with both sides in the spatial direction and size up to  $8 \times 8$  were measured every tenth iteration. Summarizing, at each value of  $\beta$ , 1100 sweeps of the  $16^3 \times 32$  lattice have been made, starting from the already thermalized configurations  $C'_1, \dots, C'_6$ , and Wilson loop factors have been measured over 100 configurations separated by 10 MC iterations each.

Let us comment briefly on our procedure. The motivation for considering a  $16^3 \times 32$  lattice is in our plan to use a few among the last configurations obtained during the long runs as well-thermalized configurations for studies of quark propagation and of the hadronic spectrum (in the quenched approximation). Large extents of the lattice in the time direction are needed for a reliable estimate of the masses. For this reason we have measured the Wilson loop factors on a  $16^3 \times 32$  lattice, rather than the  $16^4$  lattice, which would have been adequate. One might object that the full lattice will not be completely thermalized during the first iterations of the long runs and that correlations induced by the duplication of the smaller lattice may survive after the first 100 discarded iterations. But this cannot certainly affect the values for rectangular loops with both sides in the spatial direction (and indeed should not even affect the loops extending in the time direction, with a length smaller than half the original size; our restriction to spatial loops was determined mainly by programming considerations, see Sec. III). At worse, the duplication might entail some loss of statistics, which however is amply compensated by the final output of well-thermalized configurations on a lattice of large extent in time.

The results of our measurements of the Wilson loop factors are reproduced in the upper triangular part of Tables I to VI. The errors quoted are given by

$$\left[ \frac{\langle (dW_{ij})^2 \rangle}{N_c - 1} \right]^{1/2},$$

TABLE I. Results from the Monte Carlo simulation for the average plaquette action, the Wilson loop factors, and the  $X$  ratios, with  $\beta=5.6$ .

		AV. $S=0.475197(16)$ $W(I,J)*10^{**6}$							
$I/J$	1	2	3	4	5	6	7	8	
1	524 822 (58)	293 433 (77)	166 319 (74)	94 546 (62)	53 793 (53)	30 594 (45)	17 400 (40)	9913 (39)	
2	451 343 (407)	104 470 (73)	39 370 (53)	15 114 (39)	5845 (32)	2303 (30)	898 (34)	350 (33)	
3	408 154 (699)	349 055 (3601)	10 465 (46)	2913 (33)	830 (29)	260 (26)	113 (30)	65 (25)	
4	392 578 (1594)	321 588 (10 376)	272 280 (51 027)	617 (36)	108 (26)	54 (25)	15 (30)	-1 (27)	
5	386 122 (4337)	305 054 (29 326)	485 863 (237 015)	-942 491 (881 527)	49 (37)	-4 (29)	16 (28)	18 (29)	
6	367 134 (10 067)	231 437 (95 763)	-468 470 (492 532)	**	**	-63 (42)	-4 (27)	47 (26)	
7	377 741 (30 806)	-114 035 (246 419)	446 434 (2 005 278)	**	**	**	14 (35)	12 (28)	
8	379 357 (75 148)	-379 153 (387 743)	**	**	**	**	**	-12 (35)	
$I/J$	2	3	4	5	6	7	8		
		$X(I,J)*10^{**6}$							

where  $N_c (=100)$  is the total number of configurations used for the calculation and  $dW_{ij}$  is defined as

$$dW_{ij} = W_{ij} - \langle W_{ij} \rangle. \quad (2.6)$$

The lower triangular parts of the tables give the values of the  $X_{ij}$  factors, defined as

$$X_{ij} = -\ln \left[ \frac{\langle W_{ij} \rangle \langle W_{i-1j-1} \rangle}{\langle W_{i-1j} \rangle \langle W_{ij-1} \rangle} \right], \quad (2.7)$$

for  $i, j \geq 2$ . No number is quoted where any of the  $\langle W_{ij} \rangle$  on the right-hand side of Eq. (2.7) turned out to be negative, which can only be due to statistical fluctuations. The values of  $X_{ij}$  are tabulated for the convenience of the reader, and also because the computation of the statistical errors (see Sec. III) required the values of the correlations  $\langle dW_{ij} dW_{i'j'} \rangle$  which we have measured, but are too numerous to be put in print. The values for the mean-plaquette action, averaged over all 1000 sweeps and all directions (including the temporal one), are also reproduced in the tables.

We turn our attention now to the determination of the force between static quarks. (For a recent MC study of the interquark potential, on a smaller lattice, see Ref. 6.)

The potential between sources in the 3 and  $\bar{3}$  representation of SU(3) at a separation  $r = ja$  ( $a$  being the lattice spacing) is given by

$$V(r) = -\frac{1}{a} \lim_{i \rightarrow \infty} \ln \left[ \frac{\langle \langle W_{ij} \rangle \rangle}{\langle \langle W_{i-1j} \rangle \rangle} \right]. \quad (2.8)$$

(We use, in this and the following equation, double angular brackets  $\langle \langle \rangle \rangle$  to denote the true quantum-mechanical averages, as opposed to our approximations  $\langle \rangle$ .)  $V(r)$  contains a self-energy contribution; this disappears in the finite difference

$$\frac{V(r) - V(r-a)}{a} = -\frac{1}{a^2} \lim_{i \rightarrow \infty} \ln \left[ \frac{\langle \langle W_{ij} \rangle \rangle \langle \langle W_{i-1j-1} \rangle \rangle}{\langle \langle W_{i-1j} \rangle \rangle \langle \langle W_{ij-1} \rangle \rangle} \right],$$

which can be interpreted as the force  $F$  between static quarks at a separation  $r'$  somewhere between  $r-a$  and  $a$ . If  $V$  were of a purely Coulombic form,  $r'$  would be given by the geometric mean

$$r' = [r(r-a)]^{1/2} \quad (2.9)$$

TABLE II. Same as in Table I but with  $\beta=5.8$ .

		AV. S=0.432 265 (13) $W(I,J)*10^{**6}$							
I/J	1	2	3	4	5	6	7	8	
1	567 638 (52)	349 098 (66)	218 616 (71)	137 508 (63)	86 586 (59)	54 523 (53)	34 353 (46)	21 602 (41)	
2	321 658 (268)	155 643 (72)	74 519 (59)	36 421 (48)	17 921 (42)	8855 (34)	4358 (32)	2152 (33)	
3	268 469 (409)	194 777 (1175)	29 364 (54)	12 102 (37)	5054 (35)	2091 (28)	907 (30)	390 (29)	
4	252 269 (701)	170 539 (2038)	127 848 (8948)	4389 (42)	1592 (31)	601 (27)	236 (29)	100 (27)	
5	246 610 (1370)	163 938 (5424)	141 131 (17 318)	48 936 (70 133)	550 (38)	159 (26)	55 (28)	38 (28)	
6	242 461 (2395)	177 749 (11 361)	90 458 (43 236)	269 404 (161 741)	1 461 054 (3 484 590)	11 (37)	-18 (26)	31 (29)	
7	247 186 (5607)	125 513 (29 453)	99 973 (111 991)	130 671 (521 597)	**	**	29 (32)	31 (26)	
8	241 718 (10 971)	138 073 (69 098)	19 474 (279 263)	-511 552 (843 721)	**	**	127 378 (2 247 325)	30 (38)	

		$X(I,J)*10^{**6}$							
I/J	2	3	4	5	6	7	8		

and, for definiteness, we shall always use such a value as the argument for  $F$ . Thus, an approximation for  $F$  is given by

$$F(r'=[j(j-1)]^{1/2}a) = -\frac{1}{a^2} \lim_{i \rightarrow \infty} X_{ij}. \quad (2.10)$$

The difficulty in using such a formula to derive  $F$  is apparent from the tables: as  $i$  and  $j$  grow large, the corresponding  $\langle W_{ij} \rangle$  become smaller and smaller, while the magnitude of the statistical errors does not change; then the  $X_{ij}$  becomes worse and worse determined. The situation becomes particularly bad if one tries to also take large  $j$ , as needed for an evaluation of the string tension  $\sigma \equiv \lim_{r \rightarrow \infty} F(r)$ .

To achieve a reasonable estimate of  $F$  and  $\sigma$  one must strike a balance, finding a way to use the information contained in  $X_{ij}$  both for large  $i$  and  $j$ , where the value of  $X$  is, in principle, closer to the quantities one wishes to calculate, and for smaller  $i$  and  $j$ , where the precision in the determination of  $X$  is much larger, but where the relation between  $X$  and  $F$  is less direct. This requires some method of extrapolation, which will necessarily involve subjective criteria. We proceed as follows. We notice that

if, in Eq. (2.10), the roles of  $i$  and  $j$  are reversed and, instead of taking  $i \gg j$ , one considers  $i \ll j$  (provided  $j$  is large enough), the same formula will give  $F$  at separation  $r'=[i(i-1)]^{1/2}a$ . Assuming a Coulombic behavior for small  $r'$ , one expects then a behavior

$$X_{ij} \approx \frac{1}{i(i-1)} \quad (2.11)$$

for small  $i$ . The simplest possible interpolation for  $X_{ij}$  consists in assuming a superposition of a constant term and a term with a behavior as in Eq. (2.11):

$$X_{ij} \sim b_j + \frac{c_j}{i(i-1)}. \quad (2.12)$$

For all values of  $\beta$  and  $j$  we have therefore plotted the values of  $X_{ij}(\beta)$  as functions of the variable  $x = 1/i(i-1)$  and fit the points in terms of a straight line  $b + cx$ . The intercept  $b_j$  was then taken to give the extrapolation of  $X_{ij}$  for infinite  $i$ , i.e., the force  $F$  at separation  $a[j(j-1)]^{1/2}$ . Figure 1 illustrates our procedure for a definite value of  $\beta$  ( $=6.2$ ). The upper part shows the fits to the points  $X_{ij}$  at fixed  $j$  ranging from 2 to 8. In the bottom part the intercepts  $b_j$  thus obtained have been

TABLE III. Same as in Table I but with  $\beta=6.0$ .

AV. S=0.406328 (11)								
$W(I,J)*10^{**6}$								
I/J	1	2	3	4	5	6	7	8
1	593 638 (38)	383 539 (55)	252 592 (60)	167 161 (64)	110 746 (62)	73 386 (58)	48 650 (51)	32 244 (46)
2	265 482 (231)	190 020 (72)	101 256 (65)	55 181 (54)	30 280 (45)	16 649 (39)	9 152 (34)	5 054 (33)
3	211 810 (294)	141 116 (725)	46 855 (63)	22 688 (46)	11 166 (39)	5 522 (32)	2 723 (31)	1 353 (31)
4	194 212 (430)	118 212 (1229)	94 023 (3551)	10 000 (44)	4 550 (32)	2 044 (27)	966 (28)	441 (25)
5	188 411 (755)	108 821 (2542)	78 577 (55 512)	58 604 (20 395)	1 952 (42)	800 (25)	385 (26)	147 (24)
6	186 603 (1496)	105 988 (4378)	95 829 (12 962)	92 112 (36 307)	-139 889 (108 900)	377 (38)	132 (26)	31 (27)
7	187 343 (2276)	108 499 (8856)	42 349 (25 120)	-17 218 (74 867)	318 467 (204 616)	-536 870 (444 336)	79 (34)	-7 (26)
8	182 387 (4360)	105 579 (19 927)	86 012 (56 860)	178 599 (175 077)	468 804 (863 928)	**	**	-39 (34)
I/J	2	3	4	5	6	7	8	
$X(I,J)*10^{**6}$								

TABLE IV. Same as in Table I but with  $\beta=6.2$ .

AV. S=0.386286 (10)								
$W(I,J)*10^{**6}$								
I/J	1	2	3	4	5	6	7	8
1	613 653 (41)	410 181 (60)	279 506 (69)	191 382 (67)	131 237 (63)	90 000 (58)	61 733 (51)	42 349 (49)
2	233 023 (184)	217 184 (79)	123 485 (71)	71 680 (58)	41 914 (47)	24 573 (41)	14 431 (37)	8 441 (32)
3	181 056 (226)	112 395 (702)	62 746 (72)	33 212 (55)	17 838 (42)	9 639 (35)	5 224 (32)	2 818 (31)
4	165 148 (349)	92 292 (774)	75 193 (2303)	16 306 (53)	8 254 (35)	4 208 (30)	2 148 (30)	1 119 (27)
5	159 325 (509)	84 978 (1378)	59 285 (3367)	46 596 (10 243)	3 988 (44)	1 923 (31)	940 (28)	444 (28)
6	156 786 (867)	81 559 (2737)	58 138 (7062)	55 414 (14 357)	91 759 (47 439)	846 (41)	438 (28)	225 (26)
7	155 237 (1554)	80 366 (5220)	59 699 (13 046)	44 062 (32 513)	-57 731 (64 332)	-142 981 (163 561)	262 (34)	131 (26)
8	159 444 (2556)	80 843 (9322)	35 194 (25 257)	97 525 (66 881)	-83 520 (137 338)	22 133 (249 324)	-317 669 (578 429)	91 (41)
I/J	2	3	4	5	6	7	8	
$X(I,J)*10^{**6}$								

TABLE V. Same as in Table I but with  $\beta=6.4$ .

		AV. S=0.369 319 (9) $W(I,J)*10^{**6}$							
I/J	1	2	3	4	5	6	7	8	
1	630 692 (35)	432 924 (46)	302 761 (51)	212 709 (56)	149 652 (55)	105 306 (51)	74 125 (49)	52 170 (46)	
2	210 197 (166)	240 834 (60)	143 377 (57)	87 069 (52)	53 214 (46)	32 608 (39)	19 986 (36)	12 274 (34)	
3	161 015 (181)	97 126 (450)	77 457 (62)	43 534 (50)	24 844 (43)	14 239 (33)	8 164 (29)	4 702 (32)	
4	145 762 (253)	77 407 (574)	56 594 (1605)	23 121 (54)	12 522 (37)	6 873 (35)	3 833 (32)	2 093 (28)	
5	140 755 (430)	68 552 (1043)	52 378 (2034)	27 232 (5957)	6 599 (39)	3 474 (27)	1 894 (27)	1 014 (27)	
6	138 340 (717)	66 819 (1691)	43 261 (4101)	41 758 (8549)	35 254 (21 272)	17 65 (35)	950 (30)	488 (28)	
7	138 372 (1174)	66 811 (2871)	27 678 (7205)	22 383 (14 853)	12 847 (30 953)	133 003 (101 161)	448 (42)	207 (28)	
8	136 286 (1686)	64 179 (5401)	53 065 (13 372)	20 679 (26 669)	42 215 (61 470)	102 117 (147 118)	-76 085 (438 205)	104 (36)	
I/J	2	3	4	5	6	7	8		
		$X(I,J)*10^{**6}$							

TABLE VI. Same as in Table I but with  $\beta=6.6$ .

		AV. S=0.354 327 (9) $W(I,J)*10^{**6}$							
I/J	1	2	3	4	5	6	7	8	
1	645 625 (37)	453 127 (52)	323 889 (59)	232 537 (64)	167 160 (65)	120 214 (65)	86 458 (62)	62 190 (58)	
2	192 622 (140)	262 304 (67)	162 059 (66)	101 992 (58)	64 554 (53)	40 987 (46)	26 007 (39)	16 535 (35)	
3	145 773 (167)	86 346 (341)	91 842 (65)	53 945 (52)	32 111 (42)	19 284 (41)	11 551 (37)	6 920 (35)	
4	131 717 (193)	69 036 (429)	47 202 (1134)	30 225 (48)	17 226 (37)	9 950 (34)	5 702 (33)	3 274 (30)	
5	127 296 (366)	61 388 (711)	43 481 (1475)	30 365 (4251)	9 524 (43)	5 337 (32)	2 993 (28)	1 692 (30)	
6	124 568 (610)	55 638 (1236)	38 987 (2589)	30 310 (5368)	31 222 (16 377)	2 898 (41)	1 589 (30)	919 (28)	
7	125 285 (846)	57 600 (2116)	44 229 (4990)	21 568 (8916)	22 989 (19 597)	11 046 (51 449)	861 (39)	484 (28)	
8	123 428 (1381)	59 539 (3529)	42 355 (7358)	15 490 (16 761)	-23 140 (32 411)	28 335 (67 846)	-68 956 (151 285)	292 (40)	
I/J	2	3	4	5	6	7	8		
		$X(I,J)*10^{**6}$							

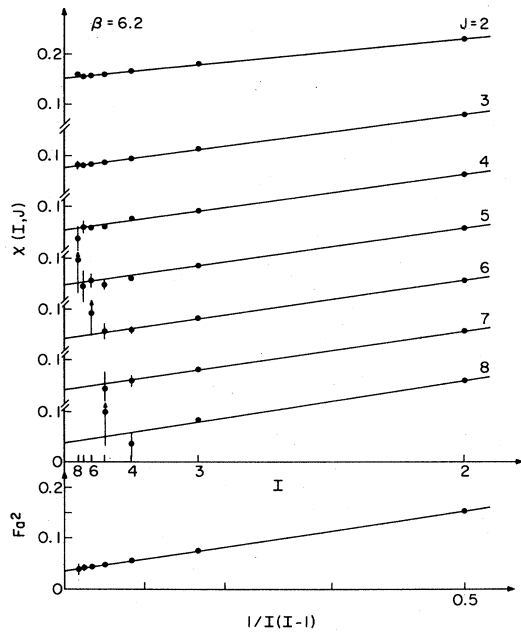


FIG. 1. The fitting procedure used to determine force and string tension at  $\beta=6.2$ .

equated to  $Fa^2$  and plotted versus  $1/j(j-1)$ . [The labeling is actually  $b_i$  versus  $1/i(i-1)$  for uniformity of notation with the upper graphs.] One expects that a fit in terms of a constant-plus-Coulombic term would give an even better extrapolation for the force than for the  $X$  factors themselves. The intercept in the lower graph has been used as an estimate of  $\sigma a^2$  at a definite  $\beta$ .

We do not claim that the fit of Eq. (2.12) should reproduce the correct functional form of the  $X_{ij}$  factors; what one needs however is not a complex, many-parameter fit to the MC data, but a simple, straightforward method of extrapolation, capable of combining the information im-

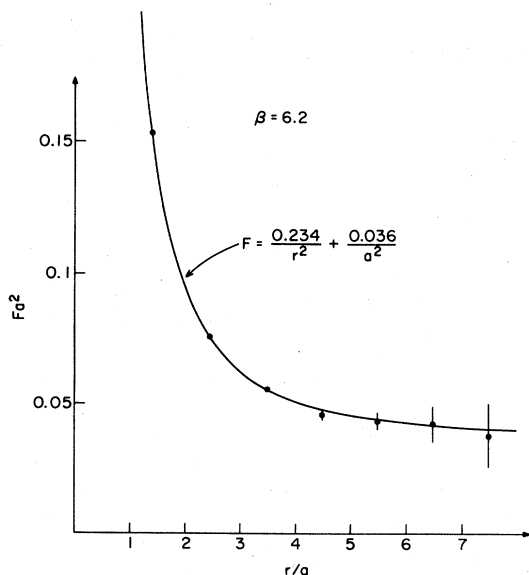


FIG. 2. Monte Carlo results for the force versus a linear-plus-Coulombic fit at  $\beta=6.2$ .

PLICIT in the Wilson loop factors for small and large loop sizes, with some appropriate weights. The consistency of the data points with the straight-line fits in Fig. 1 suggests that our procedure may be reasonable. Figure 1 is typical. We did not select the value of  $\beta$  producing the better looking graph. Larger values of  $\beta$  give generally more precise data for  $X_{ij}$ , with good agreement with a constant-plus-Coulombic behavior; the statistical errors become larger for smaller values of  $\beta$ , but the quality of the fits remains the same. The errors we reproduce are purely statistical. They do not take into account any systematic effects associated with the method of extrapolation, which would be difficult to evaluate. Our quoted errors thus measure by how much the points might be expected to vary if results from a different Monte Carlo simulation were interpolated by the same technique.

Figure 2 illustrates the results for  $Fa^2$  obtained at  $\beta=6.2$  (same data points as in the bottom graph of Fig. 1), but plotted versus  $r/a$  and on a different scale. The solid line represents the fit

$$F = \sigma + \frac{\text{const}}{r^2}.$$

In Fig. 3 we reproduce the results for the string tension obtained at the 6 values of  $\beta$  considered. The upper part of Fig. 3 gives  $\sigma a^2$ , the lower part the values for the string tension rescaled according to the expected asymptotic relation [Eq. (2.1)] between  $\Lambda$  and  $a$ , i.e.,

$$\sigma/\Lambda^2 = (\sigma a^2)/[a(\beta)\Lambda]^2.$$

The vertical scales, which are chosen to give a good resolution for  $\sigma/\Lambda^2$  and  $\Lambda/\sqrt{\sigma}$ , somehow magnify the apparent discrepancy between the numerical results and the expected asymptotic scaling behavior. The points for  $\beta=6.0, 6.2$ , and  $6.4$ , however, agree reasonably well with

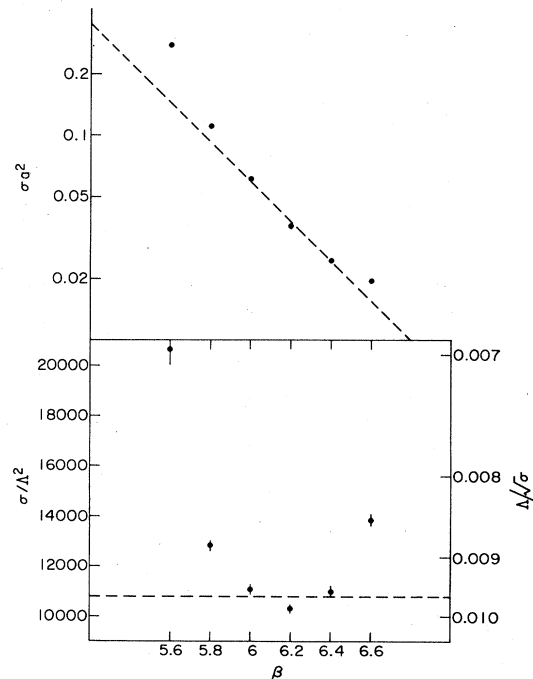


FIG. 3. Results for the string tension.

the scaling formula. The broken lines represent the scaling behavior obtained with  $\sigma/\Lambda^2=10793$ , i.e., the average of the values of  $\beta=6.0, 6.2$ , and  $6.4$ . This corresponds to a ratio  $\Lambda/\sqrt{\sigma}=9.63\times 10^{-3}$ . The fact that the point for  $\beta=6.6$  lies slightly above the scaling curve may be explained by the maximum separation being still too small to put into evidence the asymptotic behavior of the force. But for the points at  $\beta=5.6$  and  $5.8$  the maximum separation is certainly larger than the distance at which the force should become constant (see next figures) and one concludes from our results that either one is still outside the scaling domain, or that higher-order corrections to the asymptotic scaling behavior are important.

In Fig. 4 all the values found for the force are plotted in physical units of  $F/\sigma$  and  $r\sqrt{\sigma}$ , assuming for the lattice spacing  $a(\beta)$  the scaling behavior of Eq. (2.1) and for the ratio  $\Lambda/\sqrt{\sigma}$  the number quoted above. While the points for  $\beta\geq 6$  appear to lie on a universal curve, confirming scaling, the results for  $\beta=5.6$  and  $5.8$  are too high. This agrees with the deviation from the asymptotic behavior of  $\sigma$  discussed in connection with Fig. 3. However, if one rescales the numbers obtained at  $\beta=5.6$  and  $5.8$  not by the asymptotic scaling relation, but assuming for  $\sigma a^2$  the results of the numerical simulation, one obtains the graph reproduced in Fig. 5. Now all of the points agree rather well with a universal function  $F=F(\sigma)$ .

The solid line in Fig. 5 represents the expected asymptotically free behavior at short distances

$$F_c = \frac{4\alpha(r)}{3r^2} \quad (2.13)$$

with

$$\alpha(r) = \frac{4\pi}{11} [\ln(\Lambda_c r)^{-2} + \frac{102}{121} \ln \ln(\Lambda_c r)^{-2}]^{-1}. \quad (2.14)$$

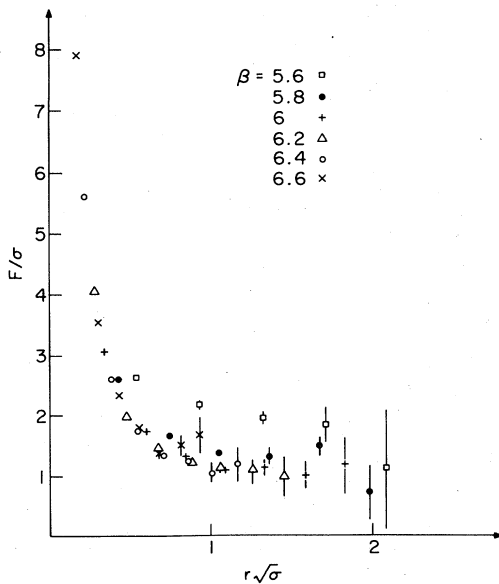


FIG. 4. Force versus separation, in physical units, assuming the asymptotic scaling formula for the relation between lattice spacing and string tension.

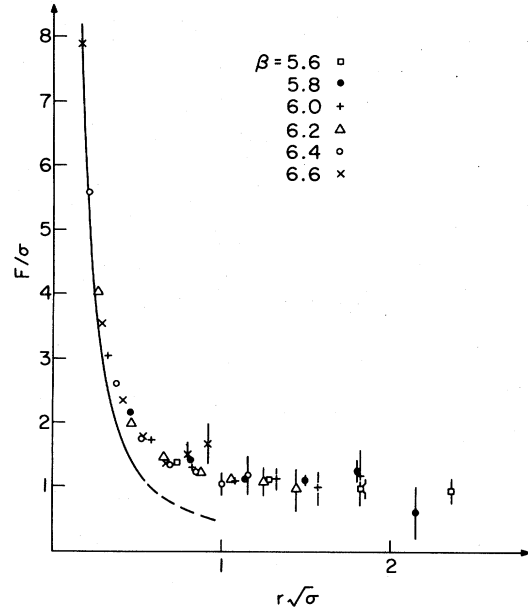


FIG. 5. Same as in Fig. 4, but with a rescaling according to the MC data for the string tension at  $\beta=5.6$  and  $5.8$ . The line represents the expected short-distance behavior.

The scale parameter  $\Lambda_c$  appearing in Eq. (2.14) can be theoretically related to the lattice scale parameter<sup>7</sup> and one finds

$$\frac{\Lambda_c}{\Lambda} \approx 30.19. \quad (2.15)$$

With our value for  $\Lambda/\sqrt{\sigma}$  this equation converts into

$$\Lambda_c \approx 0.29\sqrt{\sigma},$$

which is the value we have used in drawing the curve. The agreement between our data and the expected short-distance behavior is remarkable. One scarcely needs to emphasize that no adjustable parameter enters in the determination of the theoretical curve. The consistency we find at short distances gives strong support to the correctness of the numerical analysis.

### III. COMPUTATIONAL DETAILS

The whole calculation has been done with the CDC CYBER 205 at ICS, Fort Collins, Colorado. The code has been written so as to take full advantage of the vectorized capability of that mainframe. The characteristics of the program for the Monte Carlo simulation have been presented elsewhere.<sup>5</sup> About the calculation of the Wilson loop factors, let us mention here that our data structure is organized into sets corresponding to definite values of the time coordinate (time-slicing) which are input and output to magnetic disc as required. Thus, for the MC upgrading,  $U_x^\mu$  variables corresponding to three consecutive values (say  $t-1$ ,  $t$ , and  $t+1$ , if  $t$  is the time coordinate of the variables being upgraded) are at any moment present in fast memory, while the variables with  $t+2$  and  $t-2$  are input and output, respectively. Such data structure



makes it much less demanding, insofar as input/output operations and memory requirements are concerned, to calculate the loop factors for rectangles with both sides spacelike, than for rectangles extending in the time direction. Thus, we have limited our averages to spatial loop factors.

The calculational procedure is then straightforward: at the completion of every tenth MC iteration, in a loop over time all hyperplanes at  $t = \text{const}$  are brought into fast memory. As a first step all the transport factors corresponding to the loop sides, i.e., to segments of length up to 8, are calculated and stored in fast memory. In a subsequent step the four transport factors associated with the loops of all possible sizes up to  $8 \times 8$  are combined into the expression for  $w_{x,ij}^{\mu\nu}$ . All operations are done in fully vectorized fashion, with vector length equal to the (three-dimensional) volume of the lattice, i.e.,  $16^3$ . We have used 32-bit arithmetic, as in the MC simulation. As mentioned in Ref. 5, the effects of round-off errors are brought well below the uncertainty due to statistical fluctuation by renormalizing the  $U_x^{\mu\nu}$  matrices every few iterations (in our case 5). In particular, they are renormalized immediately

$$\rho_{ij}(l,k) = \frac{\sum_x (w_{x,ij}^{\mu\nu(k)} - \langle w_{ij} \rangle)(w_{x,ij}^{\mu\nu(k+l)} - \langle w_{ij} \rangle)}{\left[ \sum_{\substack{x \\ \mu, \nu \leq 3}} (w_{x,ij}^{\mu\nu(k)} - \langle w_{ij} \rangle)^2 \sum_{\substack{x \\ \mu, \nu \leq 3}} (w_{x,ij}^{\mu\nu(k+l)} - \langle w_{ij} \rangle)^2 \right]^{1/2}}. \quad (3.1)$$

Representative values for this quantity, evaluated over ten consecutive sweeps of the lattice, are reproduced in Table VII. One sees that the Wilson factors of loops of large size have negligible autocorrelation even after a single pass through the lattice, but that the factors for smaller loops remain substantially autocorrelated in the course of several iterations. To include into our sum quantities with some degree of statistical independence, we decided to separate the measurements of the Wilson loops by 10 MC upgradings. This also represents a reasonable balance between the amounts of CP time dedicated to the upgrading and to the measurements. Notice however that our results for the autocorrelations refer to fluctuations of the local quantities; the lattice average  $W_{ij}$  might still exhibit long-range correlations. A statistics of 100 measurements would not be sufficient to put these autocorrelations, if indeed present, into evidence. In any event, the expectation is that, because the simulation is performed away from the possible critical points (including the deconfining transition, with our size lattice), correlations with a range exceeding a few hundred MC iterations (and thus comparable to the duration of our simulation) should be highly suppressed and would not introduce applicable bias on the results.

In the course of the calculation we accumulated all of the products  $W_{ij}W_{i'j'}$ . The final sums have been used for the analysis of the statistical errors, as follows. Let us assume that the values found for the  $W_{ij}$  have a Gaussian

before the calculation of the loop factors begins. Also, one can easily convince oneself that the effect of round-off errors in the calculation of  $\langle W_{ij} \rangle$  cannot produce any significant loss of precision. Not content with the argument, we checked this point by calculating the averages over a few configurations in 64-bit arithmetic, and we found values for  $\langle W_{ij} \rangle$  never differing from those evaluated in 32-bit arithmetic by more than  $10^{-6}$  (i.e., by one unit in the least significant digit in the tables). The CP time for the calculation of all (spatial) loop factors (up to  $8 \times 8$ ) on a definite configuration is 79 sec. In the course of the upgrading, the exact value of the total action is constantly recomputed, by adding to the correct sum (initialized every few iterations) the variation induced by the change of the individual link variables.

A question which arises in most Monte Carlo simulations is how often one should measure the observables. Trying to find some guidance, we evaluated the autocorrelation of the individual loop factors. Namely, if  $w_{x,ij}^{\mu\nu(k)}$  represents the value of  $w_{x,ij}^{\mu\nu}$  [see Eqs. (2.1) and (2.2)] at the  $k$ th iteration, the autocorrelation  $\rho_{ij}(l,k)$  is defined as

distribution around the correct, quantum-mechanical averages  $\langle \langle W_{ij} \rangle \rangle$ , but that there is no statistical correlation among the errors

$$dW_{ij} \equiv W_{ij} - \langle \langle W_{ij} \rangle \rangle \quad (3.2)$$

found in the course of different measurements. Let us also denote the error of the final average by

$$d \langle W_{ij} \rangle \equiv \langle W_{ij} \rangle - \langle \langle W_{ij} \rangle \rangle, \quad (3.3)$$

and by overbars averages taken over the above-mentioned Gaussian distribution. Under these assumptions the best estimate for the quantities  $d \langle W_{ij} \rangle d \langle W_{i'j'} \rangle$  is given by

$$\overline{d \langle W_{ij} \rangle d \langle W_{i'j'} \rangle} \approx \frac{1}{N_c - 1} (\langle \overline{W_{ij} W_{i'j'}} \rangle - \langle W_{ij} \rangle \langle W_{i'j'} \rangle), \quad (3.4)$$

$N_c$  being the total number of measurements. (Let us recall that we use simple angular brackets to denote averages over measurements, e.g.,

$$\langle W_{ij} W_{i'j'} \rangle \equiv \frac{1}{N_c} \sum_k W_{ij}^{(k)} W_{i'j'}^{(k)} .$$

The quantities  $(d \langle W_{ij} \rangle d \langle W_{i'j'} \rangle)^{1/2}$  are the numbers quoted as statistical errors in the measurement of Wilson loop factors in Tables I to VI.

About the  $X$  ratios, an estimate of the error can be ob-

TABLE VII. Autocorrelation between square Wilson loops. Correlations are computed between all the square loops, at a given size, corresponding to an initial configuration and those corresponding to another configuration created by applying 1, 2, 4, 6, 8, and 10 Monte Carlo sweeps to the original configuration. The values are similar for all  $\beta$  values. Presented here are the correlation values for  $\beta=6.0$  and  $\beta=6.6$ .

No. of MC sweeps separating	Square loop size							
	1	2	3	4	5	6	7	8
	$\beta=6.0$							
1	0.343	0.304	0.200	0.113	0.058	0.036	0.020	0.010
2	0.138	0.126	0.070	0.029	0.009	0.006	0.000	0.002
4	0.037	0.038	0.017	0.004	-0.002	0.002	0.000	0.002
6	0.009	0.014	0.008	0.004	0.000	-0.002	-0.002	0.000
8	0.004	0.007	0.003	0.000	-0.001	0.003	0.001	0.001
10	0.003	0.004	0.007	0.002	0.003	0.001	-0.002	-0.001
	$\beta=6.6$							
1	0.309	0.301	0.231	0.144	0.085	0.047	0.029	0.016
2	0.115	0.117	0.085	0.044	0.019	0.011	0.006	0.001
4	0.022	0.029	0.026	0.011	0.006	-0.002	0.000	-0.001
6	0.007	0.012	0.012	0.002	0.002	0.002	0.001	-0.002
8	0.001	0.005	0.007	0.000	0.000	0.002	0.000	-0.002
10	0.000	0.003	0.003	0.000	0.000	0.000	0.000	0.000

tained assuming that the errors in the Wilson loop factors are so small that a linear expansion can be made. One finds then

$$\overline{(dX_{ij})^2} = \sum_{a,b} \frac{d\langle W_a \rangle d\langle W_b \rangle}{W_a W_b}, \quad (3.5)$$

where  $a, b$  represent pairs of indices  $\{ij\}$  and the sum runs over  $a, b = \{ij\}, \{i-1j\}, \{ij-1\}, \{i-1j-1\}$ . The numbers  $\{\overline{(dX_{ij})^2}\}^{1/2}$ , with the averages  $\langle dW_a \rangle \langle dW_b \rangle$  as in Eq. (3.4), are reproduced in the tables as statistical errors for the  $X$  ratios. These errors thus do take into account correlations between loop factors for loops of different size; of course, the expansion leading to Eq. (3.5) breaks down if the error for  $X_{ij}$  turns out comparable in magnitude to  $X_{ij}$  itself. In such cases the quoted errors have just indicative value. Negative values for the loop factors can only be produced by statistical fluctuations; if any of the  $W_{ij}$  in the formula for  $X_{ij}$  is negative, the expression does not make sense and four asterisks appear in the corresponding entry in the tables.

The fitting procedure leading to the estimate of the force and of the string tension has been done minimizing with respect to  $b_j$  and  $c_j$  the sum of the squared deviations from the line

$$X_{ij} = b_j + c_j / i(i-1),$$

weighted by the corresponding errors in  $X_{ij}$ , i.e., minimizing the form

$$Q = \sum_i \frac{\left[ X_{ij} - b_j - \frac{c_j}{i(i-1)} \right]^2}{\overline{(dX_{ij})^2}}. \quad (3.6)$$

$X$ 's with negative values have been effectively removed from the fits by assigning them an arbitrarily large error. Both  $b_j$  and  $c_j$  are given by expressions linear in the  $X_{ij}$ ; let these be of the form

$$b_j = \sum_i B_{ji} X_{ij}, \quad c_j = \sum_i C_{ji} X_{ij}. \quad (3.7)$$

Then, assuming again a Gaussian distribution for the errors  $dX_{ij}$  and neglecting this time correlations between different  $X_{ij}$ , one estimates errors

$$\begin{aligned} \overline{(db_j)^2} &= \sum_i B_{ji}^2 \overline{(dX_{ij})^2}, \\ \overline{(dc_j)^2} &= \sum_i C_{ji}^2 \overline{(dX_{ij})^2}. \end{aligned} \quad (3.8)$$

We used Eq. (3.8) to determine the errors in the force and string tension. As we have previously emphasized, these errors reflect purely statistical fluctuations, and do not take into account possible biases introduced by the extrapolation procedure.

#### IV. CONCLUSIONS

Our results constitute, we believe, a determination of the force among static quarks and of the string tension, not affected, because of the large size of the lattice, by finite-volume effects. The results are self-consistent, in the sense that the extrapolations to infinite time ( $i \rightarrow \infty$ ) lead to values of the force in good agreement, at any fixed  $\beta$ , with a Coulombic-plus-constant behavior and, moreover, for almost all of the  $\beta$  but the last ( $\beta=6.6$ ), the points at largest separation always fall in the domain

where the constant behavior has already set in (this can be seen from Figs. 4 and 5).

The string tension appears to scale in agreement with the expected asymptotic-freedom behavior for  $\beta \geq 6$ . The corresponding ratio  $\Lambda/\sqrt{\sigma}$  is larger than that found in the early MC studies of the string tension, which were limited by severe finite-size effects, and a little smaller than what would be needed to obtain good agreement with experimental values in the most recent calculations of the spectrum. However, the latter are also almost certainly affected by several approximations, including the one of neglecting internal fermionic loops, and thus the remaining discrepancy does not represent an irreconcilable inconsistency of the theory.

The results at  $\beta=5.6$  and  $5.8$  are definitely outside the domain of asymptotic scaling. It is interesting that, if the scale of forces and distances is adapted to the measured values of  $\sigma$ , the data for the force lie on the universal curve also at these two lowest values for  $\beta$ . This might indicate that scaling has already set in, although higher-order corrections are relevant in the expression for the  $\beta$  function. This might also explain why determination of observables done at values of  $\beta$  smaller than 6 seem in better agreement with a lower value for  $\Lambda/\sqrt{\sigma}$  (closer to the original determination), than the one proposed here or the even larger one suggested by some studies of the spectrum.

Another noticeable point is that, as has been remarked already, the approach to the asymptotic scaling curve is from above. This implies some activity in the curve for  $\sigma$  as a function of  $\beta$  in the region from 5 to 6, which may be attributed to the presence of a neighboring singularity in an extended coupling-constant space, where the action also contains a term in the adjoint representation of SU(3). It would be interesting to have accurate results of the string tension along lines in this space that proceed farther away from the singularity. We have adapted our code to the simulation of a system with both terms (fundamental and adjoint representations) in the action, and shall report about the results in a future publication.

*Note added.* It has been pointed out to us that it would be valuable to have an estimate of the error in our determination of the ratio  $\Lambda/\sqrt{\sigma}$ . The problem in evaluating such error is of course that, while we can quantify the errors due to statistical fluctuations and have done so, there are larger margins of uncertainty introduced by the neces-

sary extrapolation procedures, which cannot be unambiguously identified. Thus, for instance, the statistical errors induce an uncertainty

$$\Lambda/\sqrt{\sigma} = (9.84 \pm 0.08) \times 10^{-3}$$

for the ratio obtained at  $\beta=6.2$ , the lowest point in the bottom part of Fig. 3. This error, indicated by the small error bars in the same figure, is however almost certainly smaller than the error due to the fact that even the points at 6, 6.2., and 6.4 follow only approximately the scaling curve. A more realistic estimate of the error may be obtained comparing the value quoted above, i.e.,  $9.84 \times 10^{-3}$ , with the value we obtained averaging the data at  $\beta=6, 6.2, \text{ and } 6.4$ , namely,  $9.63 \times 10^{-3}$ . In a study of universality, which will be published shortly, we find, among other things, that the graphs for the force versus separation in physical units cannot discriminate between those two values for  $\Lambda/\sqrt{\sigma}$ . Thus it would be sensible to allow for an error  $\Delta(\Lambda/\sqrt{\sigma})$  of at least  $0.21 \times 10^{-3}$ . The situation becomes even less clear if one tries to estimate the true error in  $\Lambda/\sqrt{\sigma}$ , i.e., not the local degree of uncertainty in the region  $\beta \sim 6$ , but rather the difference between the value presently determined and the theoretical value that would follow from an exact calculation of  $\sigma$ , extrapolated to the continuum limit  $\beta = \infty$ . In absence of an exact calculation of  $\sigma$  (whose availability, incidentally, would detract much from the interest of the present work) the best estimate of such error comes from the comparison of numerical and theoretical values for the ratios of scales following from different choices of the action. In the study of universality mentioned above we find that those two ratios differ by about 15% for a specific choice of actions.

#### ACKNOWLEDGMENTS

We would like to thank Control Data Corporation for awarding time on the CDC CYBER 205 at the Institute for Computational Studies at Colorado State University where the computations described in the text were carried out. One of the authors (K.J.M.M.) would like to thank R. T. French and the Idaho National Laboratory for the award of a grant which made his visit to Idaho possible. This research was also carried out in part under the auspices of the U.S. Department of Energy under contract No. DE-AC02-76CH00016.

\*Permanent address: Institute for Computational Studies, Department of Mathematics, Statistics and Computing Science, Dalhousie University, Halifax, Nova Scotia, Canada B3H 4H8 and Department of Mathematics, Royal Holloway College, Englefield Green, Surrey TW20 OEX, U.K.

<sup>1</sup>M. Creutz, L. Jacobs, and C. Rebbi, Phys. Rep. **95**, 201 (1983); C. Rebbi, editor, *Lattice Gauge Theories and Monte Carlo Simulations* (World Scientific, Singapore, 1983); M. Creutz, *Quarks, Gluons, and Lattices* (Cambridge University Press, Cambridge, 1983).

<sup>2</sup>M. Creutz, Phys. Rev. Lett. **43**, 206 (1979).

<sup>3</sup>M. Creutz, Phys. Rev. Lett. **45**, 313 (1980); E. Pietarinen, Nucl. Phys. **B190**, 349 (1981); M. Creutz and K. J. M. Moriarty, Phys. Rev. D **26**, 2166 (1982); R. W. B. Ardill, M. Creutz, and K. J. M. Moriarty, *ibid.* **27**, 1956 (1983); M. Fukugita, T. Kaneko, and A. Ukawa, *ibid.* **28**, 2696 (1983); D. Barkai, M. Creutz, and K. J. M. Moriarty, *ibid.* **29**, 1207 (1984); F. Gutbrod, P. Hasenfratz, Z. Kunszt, and I. Montvay, Phys. Lett. **128B**, 415 (1983); G. Parisi, R. Petronzio, and F. Rapuano, *ibid.* **128B**, 418 (1983). N. A. Campbell, C. Michael, and P.

- E. L. Rakow, Liverpool University Report No. LTH-110, 1984 (unpublished).
- <sup>4</sup>H. Lipps, G. Martinelli, R. Petronzio, and F. Rapuano, Phys. Lett. **126B**, 250 (1983); K. C. Bowler, G. S. Pawley, and D. J. Wallace, Edinburgh University Report No. 262, 1983 (unpublished).
- <sup>5</sup>D. Barkai, K. J. M. Moriarty, and C. Rebbi, Comput. Phys. Commun. **32**, 1 (1984).
- <sup>6</sup>J. Stack, ITP-Santa Barbara Report No. 136, 1983 (unpublished).
- <sup>7</sup>A. Billoire, Phys. Lett. **104B**, 472 (1981).